Synthesis and Characterisation of end-functionalised poly(*N*-vinylpyrrolidone) additives by reversible addition-fragmentation transfer polymerisation

William N. A. Bergius,[a] Lian R Hutchings,*[a] Norazilawati Muhamad Sarih,[a,b] Richard L. Thompson,[a] Michael Jeschke[c] and Rosemary Fisher[c]

Abstract. We describe herein the synthesis of a series of multi-end functionalized poly(*N*-vinyl pyrrolidone) (PVP) additives bearing two or three C_8F_{17} fluoroalkyl (CF) groups, designed as additives to modify surface properties. The PVP additives were prepared by reversible addition-fragmentation transfer (RAFT) polymerization, with end functionality imparted via the use of CF functionalized chain transfer agents (CTAs). The resulting PVP additives, when used in modest quantities dispersed in thin films of an unmodified PVP matrix significantly reduce the surface energy, rendering their surfaces more hydrophobic and lipophobic. This is achieved by virtue of the low surface energy of the pendant C_8F_{17} end groups which cause the additive to spontaneously surface segregate during the spin coating process. The resulting thin films have been characterized by static contact angle measurements using dodecane as the contact fluid, and the impact of additive molecular weight, matrix molecular weight, the number of CF groups and additive concentration upon surface properties is reported herein. Significant increases in contact angle were observed with increasing additive concentration, up to a critical aggregation concentration (CAC). Increasing the number of CF groups (from 2 to 3); reducing additive molecular weight or increasing the matrix molecular weight, resulted in increased contact angles and hence surface lipophobicity. Rutherford backscattering (RBS) analysis was performed on films containing varying concentrations of additive, in order to quantitatively measure the near-surface fluorine concentration of these films. The results of these experiments were in excellent agreement with those obtained by contact angle analysis, confirming the surface activity and low surface energy of the additives.

Introduction

Reversible addition-fragmentation chain transfer (RAFT) polymerization is a controlled radical polymerization technique of significant and topical interest and has been used successfully to produce a vast range of controlled polymeric structures including block copolymers[1-4], branched polymers[4-7] and end-functionalized polymers[8-10]. All aspects of the RAFT polymerization mechanism including additional examples of the above described structures are reported in "*The Handbook of RAFT Polymerization"* by Barner-Kowollik[11]. We describe here the synthesis (by RAFT polymerization) and characterization of multi-end functionalized polymer additives designed to modify surface properties, exploiting a multifunctional RAFT chain transfer agent in which the functionalities are part of the "R" group of the RAFT agent. This approach, using functionalized RAFT agents, has been previously explored for the introduction of relatively simple functionalities such as hydroxyl, carboxyl and amino groups[11], and in a few cases, simple fluorinated RAFT agents carrying a single fluoroalkyl group[12,13] but to the best of our knowledge, never for the synthesis of polymeric additives with multiple end groups to modify surface properties at an air-polymer interface.

The use of low concentrations of functionalized polymer additives which are capable of surface migration is an attractive solution to the ongoing challenge/opportunity in polymer science of producing materials and products with specific (high value added) surface properties from comparatively low cost commodity polymers with desirable bulk properties, such as ease of processing, mechanical strength, electrical or thermal conductivity/resistivity and gas permeability. Low surface energy, highly fluorinated surfaces such as those achieved with poly(tetrafluoroethylene) (PTFE) possess commercially attractive properties including liquid repellence, hydrophobicity, chemical inertness and low coefficient of friction for properties such as anti-fouling finishes and release coatings to biomedical devices and filter media.[14] However, fluorinated polymers are often challenging materials to process as bulk polymers. PTFE for example, has a very high melting point, a prohibitively high melt viscosity which prevents melt processing, is practically insoluble in all common solvents and if used as a dispersion/emulsion requires high loadings of surfactants. However, for many applications the desirable surface properties can be delivered by a surface layer only a few nanometers deep and for example in crosslinked, network polymers low surface energy, fluorinated surfaces can be achieved by the use of fluorinated comonomers[15-18]. For uncrosslinked systems an attractive approach is the use of low concentrations of fluorinated additives which spontaneously surface migrate during a processing step such as spin-coating, fibre-spinning or film blowing, and presents a cost effective, hazard-free and scalable methodology for modifying the surface properties of commodity polymers.

The behaviour of end functionalised polymers carrying single fluoroalkyl (CF) group at surfaces and interfaces has been studied by several research groups, although in the main it has been shown that a single CF group has a very limited impact upon surface properties and the use of multiple CF end groups presents a more efficient and effective approach to efficient surface modification[19-26]. Thus, we have previously demonstrated that the concept of using low concentrations of end functionalized polymer additives carrying multiple (2-4) CF

groups can be very effective for the modification of surface properties and offer the possibility of generating PTFE like surface properties at very low loadings (considerably less than 1.0% (w/w) CF in the bulk). The functionalized additives behave largely like macromolecular surfactants[27,28] in so much that the functional groups are tethered to the chain-end of a polymer which is preferably identical to (or a least compatible with) the bulk polymer whose surface is to be modified. Moreover, it is a very versatile concept and a wide range of polymer additives have been prepared by a variety of polymerization mechanisms including polystyrene and poly(methyl methacrylate) by atom transfer radical polymerization[29-32] polylactide by ring opening polymerization[33], polystyrene, polyisoprene and polybutadiene by anionic polymerization[34] and polyethylene[35] via the hydrogenation of high 1,4-polybutadiene prepared by anionic polymerization. Whereas the addition of functional additives is by no means the only way to modify surface properties, the described concept has several advantages over other methods of surface modification such as plasma treatment,[14,36-38] wet chemical modification[39-41] and the application of polymeric surface coatings.[42,43] Beyond the synthesis of the low molecular weight functional additive, there is no additional waste (hazardous or otherwise), it is safe and it is comparatively cheap. Moreover, the low molecular weight polymer additive can easily be incorporated into the matrix polymer *during* a processing step; surface migration occurring whilst the polymer is still in the melt, above the glass transition or in the presence of solvent. This has been shown to be the case for both spin coating of thin films[27-35] and electrospinning of fibres.[44] The polymer additive approach offers one further advantage over the methods mentioned above in that functionalised additives, depending on the nature of the functional group, have the ability to functionalise buried interfaces as well as air-polymer surfaces. We have shown for example that polybutadiene additives with multiple polar (hydroxyl) groups migrate to and accumulate at the (buried) interface between polybutadiene and a silicon wafer.[34]

Poly(*N*-vinyl pyrrolidone) (PVP) is a widely exploited, water soluble, biocompatible polymer with a wide range of commercial applications including as an adhesive, a binder in the pharmaceutical industry, in coatings and even as a food additive. PVP can be readily polymerized with a high degree of control by RAFT polymerization[45-54], less efficiently by nitroxide mediated radical polymerization [49,55,56] and not at all by other controlled/living polymerization mechanisms due to the presence of the amide functionality. Thus PVP is an interesting (and useful) polymer to demonstrate the concept of using a functionalized RAFT agent with CF groups as part of the R group for the synthesis of end functionalized polymers.

We herein report the novel synthesis of two fluoroalkyl functionalised CTAs for use in the RAFT polymerisation of NVP, and their subsequent use in the synthesis of a range of multi-end functionalised, surface modifying PVP additives, with a range of molecular weights (5,000-50,000 g mol^{-1}), bearing two or three C_8F_{17} groups. These additives were blended with commercially available PVP and the resulting polymer blends were spin coated into thin films. The surface properties of these films were investigated primarily by means of contact angle analysis, in order to investigate the effects of additive concentration, additive type, additive molecular weight, matrix molecular weight and annealing upon surface properties. Rutherford backscattering (RBS) (using an ion beam accelerator) was also performed on a range of PVP blends incorporating varying concentrations of one additive, in

order to quantitatively measure the effect of additive concentration on the near surface elemental composition of the modified thin films, RBS results showing excellent consistency with results obtained by contact angle analysis.

Experimental

Materials

Tetrahydrofuran (HPLC Grade, Fisher Scientific) was dried and degassed over sodium wire with benzophenone indicator and freshly distilled prior to use. Dichloromethane (Analytical Grade, Fisher Scientific) was used as received unless referred to as 'dry' in which case it was freshly distilled over calcium hydride. Acetone (Analytical Grade, Fisher Scientific) was dried over 3 Å molecular sieves under a blanket of dry nitrogen overnight before use, ethyl acetate (Analytical Grade, Fisher Scientific) was used as received and in any instance of water being used it was deionised. 3-Perfluorooctyl-1-propanol (FluoroChem), carbon tetrabromide (99%, Sigma-Aldrich), triphenylphosphine (Sigma-Aldrich), 3,5-dihydroxybenzyl alcohol (99%, Sigma-Aldrich), methyl 3,4,5-trihydroxybenzoate (98%, Sigma-Aldrich), potassium carbonate (≥98%, Sigma-Aldrich), 18-crown-6 ether (≥99.5%, Sigma-Aldrich) and diphenylamine (99+% A.C.S. Reagent, Sigma-Aldrich) were stored under vacuum and otherwise used as received. Lithium aluminium hydride (95% pellets, Sigma-Aldrich) and carbon disulfide (99.9%, Acros Organics) were used as received. Sodium hydride (60% dispersion in mineral oil, Sigma-Aldrich) was washed with dry hexane (dried and degassed over calcium hydride and distilled under high vacuum) using specialist apparatus on a high vacuum / nitrogen line in order to remove mineral oil. Once washed, sodium hydride was weighed and transferred into reaction vessels under a dry nitrogen atmosphere in an MBraun MB150B-G glove box. A 100 ml stock sample of pure *N*-vinyl pyrrolidone (99+%, Sigma-Aldrich) was prepared by vacuum distillation (b.p. = 92-95˚C @ 11mm/Hg) and stored under dry nitrogen in a freezer. 1,4-dioxane (ACS reagent, Sigma-Aldrich) was freshly vacuum distilled over calcium hydride prior to use. Azobisisobutyronitrile (98%, Acros Organics) was recrystallised from 1:1 chloroform / methanol before being dried under vacuum to constant mass.

Characterisation

^{1}H NMR analysis was performed using a Bruker Avance-400 spectrometer at 400 MHz using $CDCl_3$ (100%, 99.96 atom % D, Sigma-Aldrich) as a solvent. All spectra were referenced to the C*H*Cl_3 peak at 7.27 ppm, naturally present in the $CDCl_3$ solvent. Molecular weight data was obtained using triple detection size exclusion chromatography (SEC) on a Viscotek TDA 302 with refractive index, viscosity and light scattering detectors and 2 x 300 ml PLgel 5 µm mixed C columns. Dimethylformamide (DMF) was used as the eluent at a flow rate of 1.0 ml/min and at a constant temperature of 70 °C. The light scattering detector was calibrated with a narrow molecular weight polystyrene standard purchased from Polymer Laboratories using a value of 0.990 ml/g for the dn/dc of PVP, calculated using an accurate concentration solution of PVP. Elemental analysis was performed using an Exeter Analytical, Inc. CE-440 Elemental Analyser.

Surface Analysis

Thin films were prepared by spin coating onto clean glass slides using a Cammax PRS14E photoresist spinner. All films were spin coated from 5% w/v polymer solutions in MeOH, at 3000 rpm for 1 minute to give films with a thickness of approximately 250 nm. The conditions required to achieve this approximate film thickness were optimised previously by spin coating the same PVP / MeOH solutions of varying solution concentrations onto silicon wafers at a range of speeds, and then measuring the resulting film thicknesses using a Sentech SE400 Ellipsometer (up to 200 nm film thickness) and a Sentech FTP500 White Light Interferometer (above 150 nm film thickness). Once films had been spun onto the glass slides they were allowed to air dry before being dried under vacuum to constant mass. Contact angle measurements were obtained using dodecane (≥99%, Sigma-Aldrich) as the contact fluid on a Ramé-Hart NRL contact angle goniometer (model number 100-00-230), taking the average result of six measurements taken from both sides of three separate drops of dodecane deposited on the surface from a vertically held syringe. To avoid overcrowding, each graphical representation of any contact angle data contains only a single error bar, which corresponds to the average of the standard deviations for each individual data point in that data set.

Rutherford backscattering analysis

Rutherford backscattering (RBS) analysis was performed on a series of polymer films in order to investigate the near surface elemental fluorine concentration, and its relationship to overall additive concentration in the blend. Polymer films were prepared in the same way as for those used in contact angle experiments, but the films were spin coated onto clean silicon wafers and from 10% w/v polymer solutions in MeOH in order to give films with a thickness of approximately 550 nm (measured as above by interferometry). Thicker films were required in order to ensure that recoiling 4He+ from the heavier elements in the substrate were sufficiently reduced in energy that they did not overlap with the 4He+ ions recoiling from fluorine at the polymer film surface. RBS was performed using an NEC 5SDH Pelletron accelerator, and a 1.3 MeV $^4He^+$ beam was brought incident onto the sample surface at an angle of 85.4° (4.6° grazing angle). Backscattered $^4He^+$ ions were detected at 170° to the incident beam, and data was summed over 12 measurements of 2μC $^4He^+$ on different areas of the sample surface in order to minimize potential beam damage.

Synthesis of functionalized RAFT chain transfer agents

1-Bromo-3-perfluorooctyl propane (PFP-Br) (1).

1 was prepared according to a previously reported procedure,[31] by the bromination of 3-perfluorooctyl-1-propanol (PFP-OH) using carbon tetrabromide / triphenylphosphine (CBr_4 / PPh_3) in dry THF / DCM ('Appel reaction'). ^{1}H NMR (400MHz, $CDCl_3$, δ, ppm) 2.08-2.37 (m, 4H, $CH_2CH_2CH_2Br$), 3.48 (t, *J* 6.2 Hz, 2H, $CH_2CH_2CH_2Br$).

3,5-(Di-3-(perfluorooctyl)propyloxy)benzyl alcohol (DPFPB-OH) (2).

2 was prepared according to a previously reported procedure,[31] by the reaction of **1** with 3,5-dihydroxybenzyl alcohol in dry acetone, in the presence of potassium carbonate and 18-crown-6 ('Williamson ether synthesis'). ^{1}H NMR (400MHz, $CDCl_3$, δ, ppm) 1.56 (s, 1H, -CH_2OH), 2.10 (m, 4H, $CF_2CH_2CH_2CH_2O$), 2.31 (m, 4H, $CF_2CH_2CH_2CH_2O$), 4.03 (t, *J* 5.9

Hz, 4H, $CF_2CH_2CH_2\mathit{CH_2}O$), 4.64 (s, 2H, -$\mathit{CH_2}$OH), 6.37 (t, *J* 2.2 Hz, 1H, Ar*H*), 6.53 (d, *J* 2.3 Hz, 2H, Ar*H*).

3,5-(Di-3-(perfluorooctyl)propyloxy)benzyl bromide (DPFPB-Br) (3).

3 was prepared according to a previously reported procedure,[31] by the bromination of **2** using carbon tetrabromide / triphenylphosphine (CBr_4 / PPh_3) in dry THF / DCM ('Appel reaction'). ^{1}H NMR (400MHz, $CDCl_3$, δ, ppm) 1.98-2.09 (m, 4H, $CF_2CH_2\mathit{CH_2}CH_2O$), 2.15-2.22 (m, 4H, $CF_2\mathit{CH_2}CH_2CH_2O$), 3.95 (t, *J* 5.9 Hz, 4H, $CF_2CH_2CH_2\mathit{CH_2}O$), 4.36 (s, 2H, -$\mathit{CH_2}$Br), 6.41 (t, *J* 2.2 Hz, 1H, Ar*H*), 6.49 (d, *J* 2.2 Hz, 2H, Ar*H*

Methyl-3,4,5-(tri-3-(perfluorooctyl)propyloxy)benzoate (TPFPB-COOMe) (4).

4 was prepared according to a previously reported procedure,[31] by the reaction of **1** with methyl-3,4,5-trihydroxybenzoate in dry acetone, in the presence of potassium carbonate and 18-crown-6 ('Williamson ether synthesis'). ^{1}H NMR (400MHz, $CDCl_3$, δ, ppm) 2.01-2.10 (m, 2H, $CF_2CH_2\mathit{CH_2}CH_2O$), 2.10-2.20 (m, 4H, $CF_2CH_2\mathit{CH_2}CH_2O$), 2.26-2.45 (m, 6H, $CF_2\mathit{CH_2}CH_2CH_2O$), 3.92 (s, 3H, C(=O)$OCH_3$), 4.09 (t, *J* 5.9 Hz, 2H, $CF_2CH_2CH_2\mathit{CH_2}O$), 4.13 (t, *J* 5.8 Hz, 4H, $CF_2CH_2CH_2\mathit{CH_2}O$), 7.30 (s, 2H, Ar*H*).

3,4,5-(Tri-3-(perfluorooctyl)propyloxy)benzyl alcohol (TPFPB-OH) (5).

Compound 5 was prepared according to a previously reported procedure,[31] by the reduction of **4** from an ester to a primary alcohol using lithium aluminium hydride ($LiAlH_4$) in dry THF. ^{1}H NMR (400MHz, $CDCl_3$, δ, ppm) 1.66 (t, *J* 5.8 Hz, 1H, Ar-$CH_2O\mathit{H}$), 1.99-2.10 (m, 2H, $CF_2CH_2\mathit{CH_2}CH_2O$), 2.10-2.20 (m, 4H, $CF_2CH_2\mathit{CH_2}CH_2O$), 2.26-2.49 (m, 6H, $CF_2\mathit{CH_2}CH_2CH_2O$), 3.99 (t, *J* 5.9 Hz, 2H, $CF_2CH_2CH_2\mathit{CH_2}O$), 4.09 (t, *J* 5.9 Hz, 4H, $CF_2CH_2CH_2\mathit{CH_2}O$), 4.63 (d, *J* 5.7 Hz, 2H, Ar-$\mathit{CH_2}$OH), 6.60 (s, 2H, Ar*H*).

3,4,5-(Tri-3-(perfluorooctyl)propyloxy)benzyl bromide (TPFPB-Br) (6).

6 was prepared according to a previously reported procedure,[31] by the bromination of **5** using carbon tetrabromide / triphenylphosphine (CBr_4 / PPh_3) in dry THF / DCM ('Appel reaction'). ^{1}H NMR (400MHz, $CDCl_3$, δ, ppm) 1.98-2.08 (m, 2H, $CF_2CH_2\mathit{CH_2}CH_2O$), 2.10-2.20 (m, 4H, $CF_2CH_2\mathit{CH_2}CH_2O$), 2.26-2.46 (m, 6H, $CF_2\mathit{CH_2}CH_2CH_2O$), 4.01 (t, *J* 5.8 Hz, 2H, $CF_2CH_2CH_2\mathit{CH_2}O$), 4.09 (t, *J* 5.8 Hz, 4H, $CF_2CH_2CH_2\mathit{CH_2}O$), 4.44 (s, 2H, Ar-$\mathit{CH_2}$Br), 6.63 (s, 2H, Ar*H*). Elemental analysis calculated for $C_{40}H_{22}BrF_{51}O_3$: C, 30.04; H, 1.39; Br, 5.00; F, 60.58. Found: C, 30.28; H, 1.35; Br, 2.96; F, 59.41.

***S*-3,5-(di-3-(perfluorooctyl)propyloxy)benzyl-*N,N*-diphenyldithiocarbamate (DPFPB-DPCM) (7).**

7 was prepared via the following procedure. Diphenylamine (0.753 g, 1.00 equivs, 4.45 mmol) was placed in a flask, sealed with a rubber septum and flushed with dry nitrogen. 25 ml anhydrous dimethyl sulfoxide and 12.5 ml dry tetrahydrofuran was cannulated into the flask and the diphenylamine solution was then added by means of cannulation to a suspension of sodium hydride (0.107 g, 1.00 equivs, 4.45 mmol) in a 12.5 ml dry tetrahydrofuran at 0°C contained within a two-necked 500 ml round bottomed flask equipped with a magnetic stirrer, reflux condenser under a blanket of dry nitrogen. The mixture was stirred for 1.5 hours at 0°C to give a clear green solution. Carbon disulfide (0.407 g, 1.20 equivs, 5.34 mmol, 322 μl) was

then added to the solution at 0°C and the mixture stirred for a further 30 minutes to obtain an orange-yellow solution of the sodium salt of diphenyldithiocarbamate. **3** (DPFPB-Br) (5.00 g, 1.00 equivs, 4.45 mmol) dissolved in a minimum amount of dry tetrahydrofuran under dry nitrogen was cannulated into the reaction mixture, still at 0°C, and then brought slowly up to room temperature and left to stir overnight under a blanket of dry nitrogen. The reaction mixture was then partitioned between diethyl ether and water and washed a further two times with water. The organic layer was collected, dried over magnesium sulphate, filtered and then evaporated to dryness. The residue was recrystallised several times from diethyl ether to obtain the pure product as a light yellow powder in 48% yield. ^{1}H NMR (400MHz, $CDCl_3$, δ, ppm) 2.04-2.16 (m, 4H, $CF_2CH_2CH_2CH_2O$), 2.22-2.41 (m, 4H, $CF_2CH_2CH_2CH_2O$), 4.00 (t, *J* 5.9 Hz, 4H, $CF_2CH_2CH_2CH_2O$), 4.44 (s, 2H, CS(=S)CH_2), 6.33 (t, *J* 2.3 Hz, 1H, Ar*H*), 6.52 (d, *J* 2.2 Hz, 2H, Ar*H*), 7.39-7.44 (m, 10H, Ar*H*). Elemental analysis calculated for $C_{42}H_{27}F_{34}NO_2S_2$: C, 39.17; H, 2.11; N, 1.09; S, 4.98; Found: C, 39.01; H, 2.00; N, 0.84; S, 4.25.

_S_-3,4,5-(tri-3-(perfluorooctyl)propyloxy)benzyl-_N,N_-diphenyldithiocarbamate (TPFPB-DPCM) (8).

8 was prepared according to the same procedure as described above for **7**, but using **6** (TPFPB-Br) in place of **3** (DPFPB-Br). ^{1}H NMR (400MHz, $CDCl_3$, δ, ppm) 1.96-2.05 (m, 2H, $CF_2CH_2CH_2CH_2O$), 2.05-2.15 (m, 4H, $CF_2CH_2CH_2CH_2O$), 2.23-2.43 (m, 6H, $CF_2CH_2CH_2CH_2O$), 3.96 (t, *J* 5.9 Hz, 2H, $CF_2CH_2CH_2CH_2O$), 4.04 (t, *J* 5.9 Hz, 4H, $CF_2CH_2CH_2CH_2O$), 4.43 (s, 2H, CS(=S)CH_2), 6.58 (s, 2H, Ar*H*), 7.39-7.45 (m, 10H, Ar*H*). Elemental analysis calculated for $C_{53}H_{32}F_{51}NO_3S_2$: C, 36.09; H, 1.83; N, 0.79; S, 3.64. Found: C, 35.85; H, 1.72; N, 0.70; S, 3.38.

Synthesis of end-functionalized polymer additive

All additives were polymerised by means of reversible addition-fragmentation transfer (RAFT) polymerisation using the novel, functionalised chain transfer agents, **Compound 7** and **Compound 8**, and azobisisobutyronitrile (AIBN) as an initiator.

Poly(*N*-vinylpyrrolidone) additives bearing two C_8F_{17} end groups. A typical RAFT polymerisation was performed as follows: 1.00 ml NVP (1.045 g, 9.40 mmol), 1 ml 1,4-dioxane, the appropriate amount of CTA (**Compound 7**) and therefore target molecular weight was calculated by equation 1 below, and initiator (AIBN) (1:8 molar ratio AIBN:CTA) were placed in a Schlenk tube. The Schlenk tube was sealed, the contents thoroughly degassed by repeated freeze-pump-thaw cycles, then flooded with a dry nitrogen atmosphere. The contents were heated to 80°C with efficient stirring for a period of 15 hours. After being allowed to cool to room temperature, the reaction mixture was dissolved in a minimum amount of DCM if required, and poured into a 20 × volume excess of diethyl ether in order to recover the polymer by precipitation. The resulting polymer was collected by vacuum filtration. If necessary the polymer product was re-dissolved and precipitated until purity was verified by ^{1}H NMR spectroscopy.

Equation 1:

$$[\mathrm{RAFT}]_0 = \frac{[\mathrm{M}]_0 \times \mathrm{M_M} \times \mathrm{x}}{\mathrm{M_n} - \mathrm{M_{RAFT}}}$$

Where $\mathbf{[RAFT]_0}$ is the initial concentration of CTA, $\mathbf{[M]_0}$ is the initial concentration of monomer, $\mathbf{M_M}$ is the molar mass of the monomer, **x** is a decimal between zero and one representing the assumed fractional conversion of monomer into polymer, $\mathbf{M_n}$ is the target molecular weight of polymer being produced and $\mathbf{M_{RAFT}}$ is the molar mass of the CTA.

For example for the polymerisation of 2CFPVP6K (where 2CF indicates 2 C_8F_{17} groups and 6K refers to the molecular weight of the PVP polymer chain, M_n = 6,000 g mol^{-1}) – for a target molecular weight: 6,000 g mol^{-1}, and using an approximate conversion of 55% obtained from a series of previous RAFT polymerisations of *N*-vinyl pyrrolidone using a molecularly analogous dendritic CTA (G1-CTA, figure 1): 1 ml NVP, 1 ml 1,4-dioxane.

$$[\text{RAFT}]_0 = \frac{4.7004 \times 111.16 \times 0.55}{6000\text{-}1287.74} = 0.06098 \text{ mol dm}^{-3} \text{ CTA (Compound 7)}$$

Thus 0.15706g (0.12197 mmol) Compound 7 was required, and an eighth the molar amount (0.015246mmol) of AIBN = 0.00250g).

Poly *N*-vinyl pyrrolidone additives bearing three C_8F_{17} end groups. These additives were prepared in the same way as their di-functional counterparts, as described above, though using **Compound 8** as the CTA. However, due to the limited solubility of the more heavily fluorinated **Compound 8**, for target molecular weights of less than 25,000 g mol^{-1} (thus requiring larger quantities of CTA), it was necessary to use up to 100% extra solvent.

Results and discussion

Synthesis of end functionalised polymer additives

We have previously described the synthesis of a number of similar polymer additives by atom transfer radical polymerisation[29-32] and ring opening polymerisation[33] in which the multi-functional end group was introduced through the use of a functionalised initiator. We have also previously described a synthesis of analogous additives by living anionic polymerisation and subsequent endcapping, necessitated by anionic polymerisation's sensitivity to functionality and impurities.[34] Due to the amide group present in the NVP monomer, it is incompatible for use with living cationic or living anionic polymerisation. Additionally this monomer is incompatible with ATRP due to its tendency to form complexes with transition metal catalysts. Thus it was not until relatively recently that PVP has been made in a controlled fashion using controlled radical polymerisation techniques such as RAFT[48-54] and NMP,[49] mechanisms with a high tolerance towards impurities and functional groups, in addition to a wide range of temperatures and solvents. RAFT was therefore chosen as an efficient methodology for the synthesis of the end functionalised polymers described herein, exploiting the use of functionalised CTAs to impart end functionality to the nascent polymer. Di-functional (**3**) and tri-functional (**6**) fluoroalkyl moieties were synthesised according to

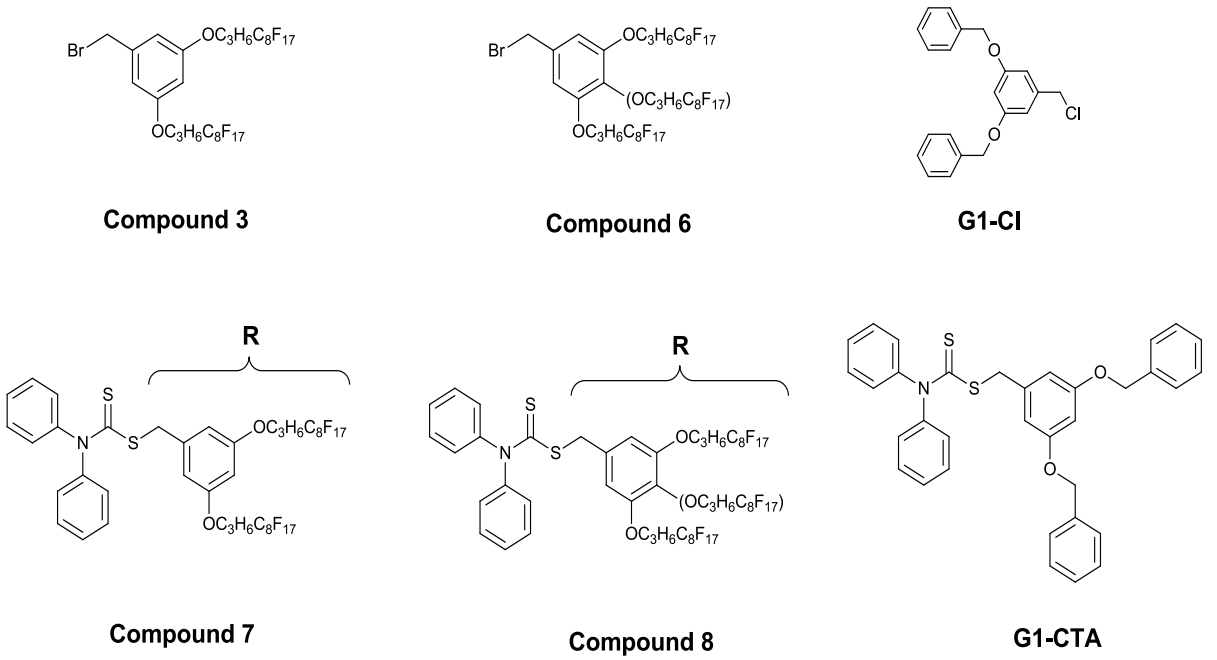

Figure 1. Chemical structure of end group precursors and CTAs.

previously published procedures[31] which were then converted into difunctional and trifunctional CTAs (**7** and **8**, Figure 1) according to the method shown in Scheme 1. NMR spectra pertaining to the synthesis of compounds **3**, **6**, **7** and **8** are included as electronic supporting information. As can be seen in step 3 of the general RAFT mechanism shown in Scheme 2, after the thermally initiated generation of free radical species from AIBN, it is the R group of the CTA which reinitiates polymerisation thus becoming the end group of the nascent polymer chain. By using a reduced concentration of AIBN relative to that of the CTA

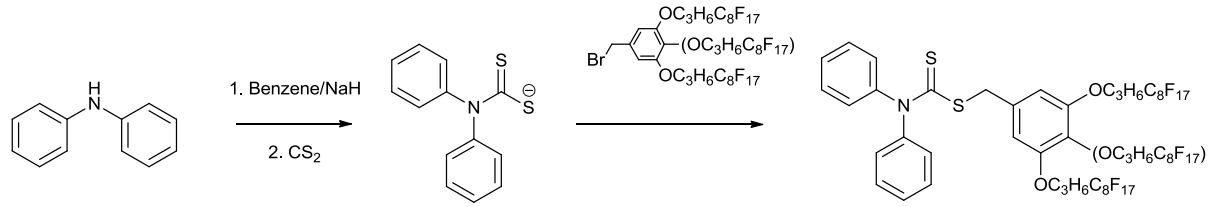

Scheme 1. Synthesis of CTA carrying three fluoroalkyl groups, TPFPB-DPCM (**8**)

only a small percentage of polymer chains are end-capped with the cyanoisopropyl AIBN residue, with up to 82% R group end-functionalisation being achieved in this work. While both compounds **7** and **8** are arguably similar CTAs, a minor complication was encountered with the use of **Compound 8**. Diminished solubility of **8,** presumably as a consequence of the CTAs high molar fluorine content, was experienced in most potential solvents, including 1,4-dioxane which was used in these polymerisations. For low molecular weight polymerisations (<25,000 g mol^{-1}) necessitating the use of larger quantities of CTA, 50-100% additional solvent was required in order to achieve full dissolution of the CTA, without which the polymerisation proceeded

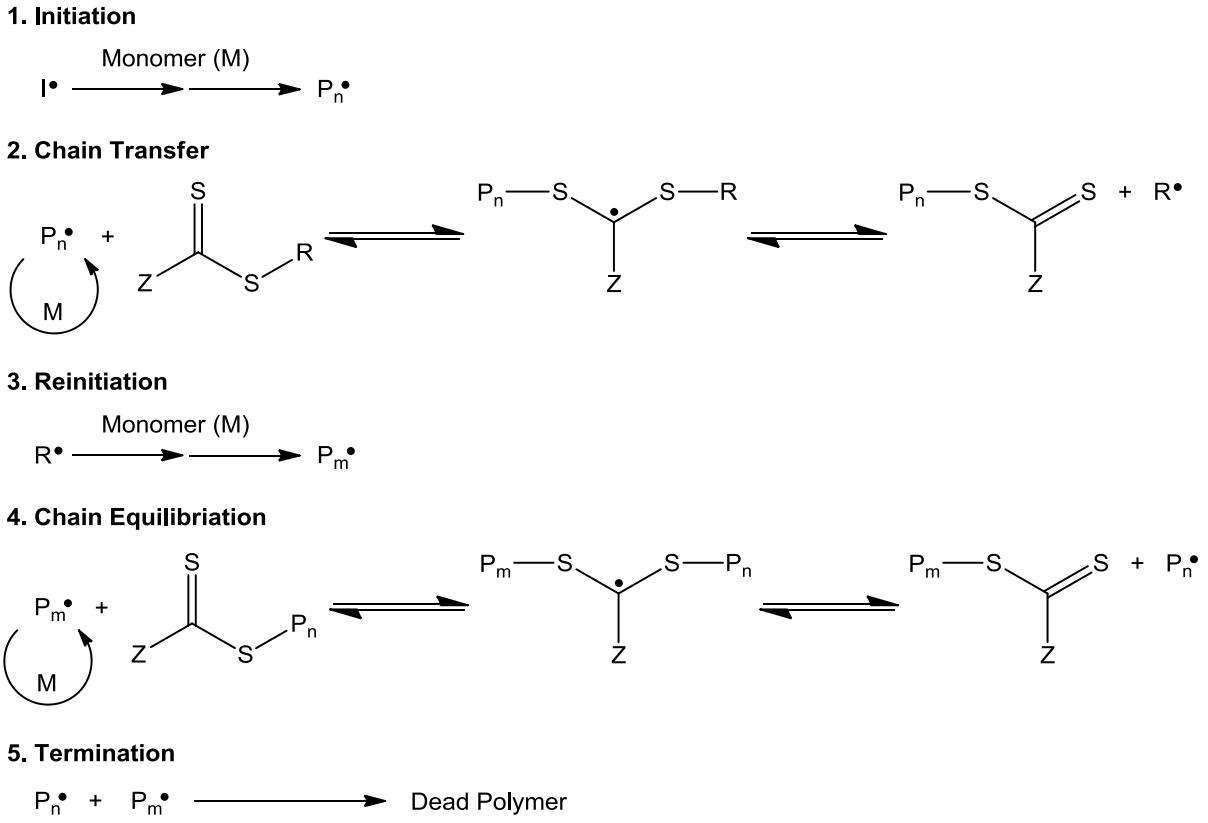

Figure 2. General mechanism for RAFT mediated polymerisation.[57]

with severely diminished control over molecular weight and polydispersity. Good agreement was achieved between target and actual number average molecular weight for both CTAs, compounds **7** and **8**, although some discrepancy did occur in some higher molecular weight cases – see table 1. It is possible that the discrepancy at higher molecular weight is due to lower conversions/incomplete reaction since the same reaction time was used for all polymerisation reactions. Dispersity index values for the difunctional CTA were acceptable (1.19 – 1.34) however for the trifunctional CTA they were higher (1.29 – 1.83) possibly as a consequence of the reduced solubility of this CTA. Yields of functionalised polymer were in the region of 40-60% which is on the low side for a RAFT polymerisation and in part this may be explained by problems associated with efficient recovery of polymer on a small scale – polymerisations were carried out on a 1g scale. However, it is likely that conversions were less than quantitative. In general the control of the polymerisation was acceptable for the difunctional CTA but far from perfect for the trifunctional CTA. Preliminary RAFT polymerisations were also carried out using a novel unfunctionalised CTA in which the R group was a first generation Frechét-type benzyl aryl ether dendron (G1-CTA – Figure 1). The synthesis of G1-CTA from G1-Cl is described in electronic supporting information. The unfunctionalised G1-CTA behaved very similarly to the difunctional CTA (7) in so much that agreement between target and actual molecular weights were good and dispersity values were acceptable (1.27 and 1.36) – see table SI, electronic supporting information. It would appear as if the R group in these two cases

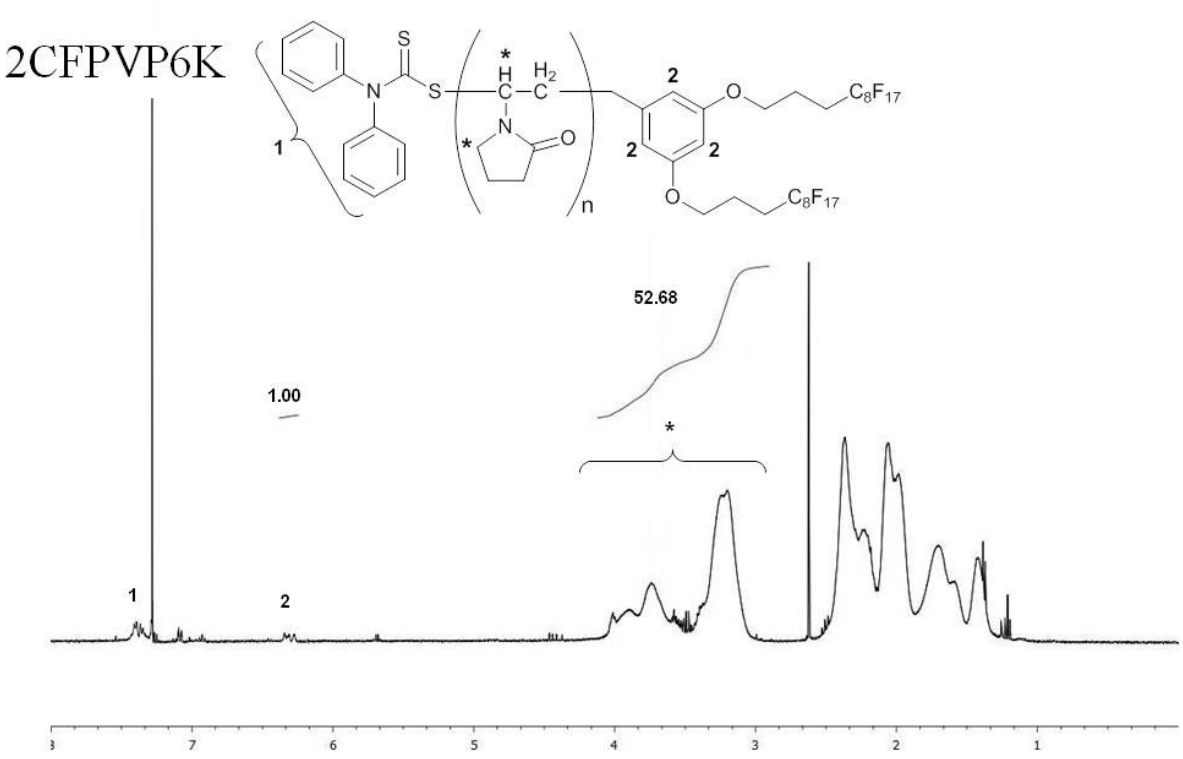

Figure 3. ^{1}H NMR spectrum (in $CDCl_3$) of the 2CFPVP6K functional additive. Of particular note are the peaks ascribed to the ten Z group aromatic protons at 6.4 ppm and the three R group aromatic protons (2) at approximately 6.25 ppm.

imparts reasonable control over the polymerisation and we can be sure that the polymerisation is proceeding via a RAFT mechanism as a result of the presence of the R group residue on the chain end – as evidenced by ^{1}H-NMR (figure 3). Of course the R group and the stability of its radical species generated in the RAFT process play an important role in the effectiveness of any CTA,[11] which becomes somewhat more unpredictable with more exotic R groups such as these. In the case of the difunctional CTA and the G1 CTA the fluoroalkyl ether groups are meta to the resultant benzyl radical and therefore unlikely to impact upon the stability of the radical which will likely behave as common benzyl radical. However in the case of the trifunctional CTA, the third fluoroalkyl group is para substituted and therefore able to directly impact upon the stability of the radical by conjugation. Although the fluorinated segment is probably too remote to have any significant effect by induction, the ether linkage is electron-releasing is likely to alter the electronic nature the benzyl radical – making the radical more electron rich than the analogous benzyl radical in the disubstituted CTA. It is possible that this also partially responsible for the higher dispersity values observed for polymerisations using the trifucntional CTA. The extent of end capping arising as a result of re-initiation from the R group was estimated by ^{1}H NMR spectroscopy by comparing the relative intensity of the peaks corresponding to the aromatic protons on the R group (indicated '2' figure 3) and two protons on the polymer repeat unit (indicated '*' figure 3) appearing between 3.0 and 4.2 ppm and using values of M_n calculated

by triple detection size exclusion chromatography (see figure 3 and table 1). Values of between 65% and 82% R

Additive[a]	Target M_n / g mol^{-1}	M_n[b] / g mol^{-1}	M_n / M_w	Yield	% Functionalisation[c]
3CFPVP6K	5,000	5,550	1.57	46%	82%
3CFPVP7K	7,000	7,150	1.45	41%	65%
3CFPVP10K	10,000	9,700	1.83	43%	54%
3CFPVP17K	20,000	17,400	1.49	39%	-
3CFPVP18K	25,000	18,000	1.29	39%	-
3CFPVP33K	50,000	33,100	1.57	53%	-
3CFPVP56K	100,000	56,100	1.37	42%	-
2CFPVP5K	6,000	5,400	1.19	37%	74%
2CFPVP6K	6,000	5,950	1.22	46%	79%
2CFPVP8K	10,000	7,950	1.20	57%	67%
2CFPVP12K	15,000	11,850	1.23	49%	71%
2CFPVP18K	25,000	18,050	1.34	46%	-
2CFPVP38K	50,000	37,850	1.28	38%	-

Table 1 Molecular weight and percentage end functionalisation for a series of PVP additives bearing two or three C_8F_{17} fluoroalkyl groups

[a] Denoted 'X'CFPVP'Y'K' where 'X' refers to the number of C_8F_{17} fluoroalkyl chains present in the end group and 'Y' refers to the $M_n \times 10^{-3}$ g mol^{-1} of the additive.
[b] M_n as determined by triple detection SEC
[c] Percentage end functionalisation calculated using ^{1}H NMR spectroscopy

group initiation and therefore fluoroalkyl end-capping were obtained for additives with a molecular weight below 9,500 g mol^{-1}. It is to be expected that the degree of R group end-functionalisation will be less than quantitative for RAFT polymerisation since a proportion of chains will always be initiated by the radical initiator – AIBN in this case. The values obtained are not unexpected for a RAFT polymerisation performed with a 1:8 ratio of initiator to CTA, as used in this work. However, for the polymer additives with higher molecular weight ascertaining the proportion of polymer chains carrying the functional R group becomes impossible to measure with any accuracy by NMR due to the diminishing intensity of the small signal attributable to the two or three aromatic protons used to establish the presence of the fluoroalkyl end group. It was possible to observe these signals but not to quantify their intensity with confidence. It should be noted that even for the lower molecular weight additives the intensity of the peak corresponding the aromatic protons on the R group are small. However, given the relative consistency of the extent of R group end-capping on the lower molecular weight additives and the subsequent surface characterisation data we have no reason to believe that the extent of end capping in these cases is outside the range observed.

Analysis of surface properties

As previously discussed, the end functionalised PVP polymer additives were designed and prepared for use, in low concentrations, as surface modifying additives in a blend with

otherwise unfunctionalised PVP. The merit of this approach to surface functionalisation lies in its ability to efficiently modify the surface properties of PVP, with only a small amount of additive, without compromising the bulk properties of the polymer and with no additional processing step. Static contact angle measurements using a goniometer and the Sessile Drop Technique[58] is a convenient method for investigating the surface properties (in this case lipophobicity, which in turn is an indicator of surface energy) of PVP films incorporating either of the two classes of additives in varying concentrations. It should be noted at this point that the concentration of additive used in the following studies assumes 100% end capping. Clearly this is not the case! In reality we would assume that in most cases the degree of functionalisation is approximately 80% based on the data for the lowest molecular weight polymer additives for which we can have the greatest confidence in the NMR data. So in figure 4a-d, the weight percent additive actually corresponds to the weight percent of low molecular weight polymer added of which we would assume about 80% is end functionalised with the fluoralkyl group derived from the R group of the CTA. However, whilst small errors probably do exist as a result of this assumption, in the majority of the analysis this small error will be irrelevant. The data presented in figure 4a-c only uses a single additive and whilst the absolute concentration of functionalised additive may be in error by a few percent it is the trend in data that is of prime concern. Only in figure 4d, where we draw comparisons between additives of different molecular weight may these small errors be an issue, however the trends displayed in figure 4d are entirely consistent with our previous studies and therefore we can conclude that our assumptions about the degree and consistency of end capping are valid.

Static contact angle measurements enable the facile investigation of surface properties of a range of polymer films, allowing direct comparisons to be made between effects arising from the concentration of additive, molecular weight of the polymer matrix, molecular weight of the functionalised additive, the number of fluoroalkyl groups on the additive and where appropriate, annealing temperatures and times. Thin films (~250nm) of PVP containing varying weight percentages of additive were spin coated on to glass slides and contact angles were measured using dodecane as the contact fluid. One of the variables investigated was the molecular weight of the PVP (unfunctionalised) matrix used in these thin films and the molecular weights of the various matrices used are shown in Table 2. Rutherford backscattering ion beam analysis (RBS) was also performed on a set of PVP films (~500nm film thickness, spin coated on to a silicon wafer) containing varying concentrations of additive, in order to quantitatively analyse the effect of additive concentration on the near surface fluorine enrichment of the film surface.

Contact angle analysis

Static contact angles data with dodecane as the contact fluid are shown in figure 4. Although it is most common to measure contact angles with water as the contact fluid, that was not possible in this case as PVP is a water soluble polymer - dodecane (a non-solvent for PVP) was therefore used as the contact fluid. A variety of different parameters have been investigated including the effect of matrix molecular weight, the effect of the number of CF groups and the impact of additive molecular weight upon surface properties. However, the

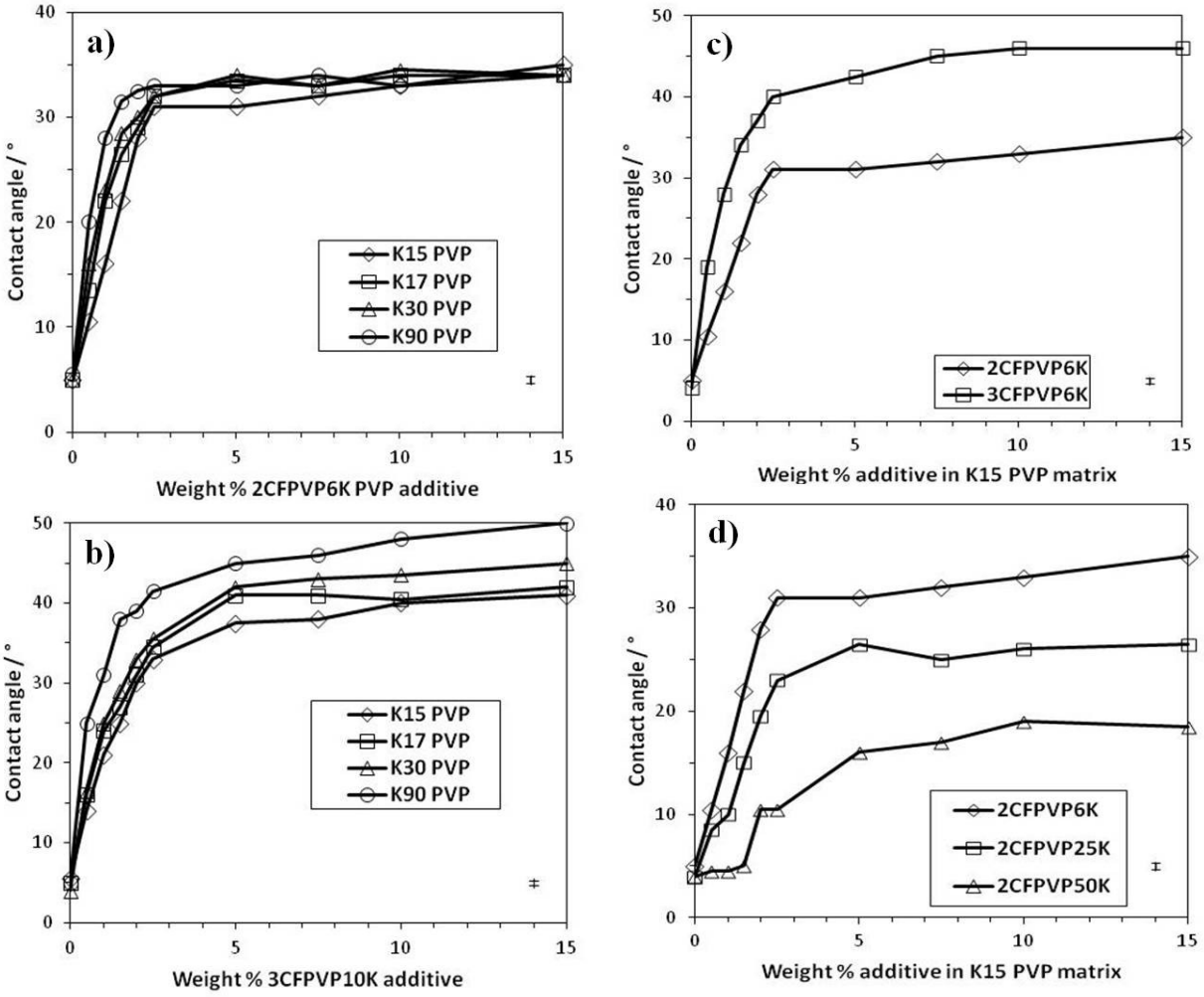

Fig. 4 Contact angle data (dodecane) as a function of additive concentrations of (a) 2CFPVP6K additive in PVP matrices of varying M_n (b), 3CFPVP10K PVP additive in PVP matrices of varying M_n, (c) of 2CFPVP6K and 3CFPVP6K in a K15 PVP matrix, (d) 2CF additives of varying M_n in a K15 PVP matrix (d).

Table 2. Molecular weight of the PVP matrices used

PVP Matrix	M_n[a] / g mol^{-1}
'K15' PVP	6,600
'K17' PVP	32,650
'K30' PVP	64,400
'K90' PVP	366,000

[a] M_n as determined by triple detection SEC

fundamental variable which has probably the biggest impact upon surface properties is the concentration of additive. It can clearly be seen in plots (4a) to (4d), that there is a common trend for contact angles to increase sharply with additive concentration (in all cases) at lower

concentrations, until a plateau region is observed, whereupon further increases in additive concentration have little or no observable impact upon contact angle, and hence surface properties. The increase in contact angle is due to the spontaneous surface segregation of the low surface energy additive during the spin-coating process, and subsequent fluorine enrichment at the surface. At low concentrations, an increase in additive concentration leads to a greater degree of fluorine enrichment at the surface and higher contact angles. One might be forgiven for interpreting the plateau region as indicating surface saturation of the additive. However, previous work[27,28] has shown that the situation is in fact more complicated than this. We have previously described a simple model to describe the behaviour of such end-functionalised additives in thin films and draw an analogy with surfactants. As such we believe that when the films are above the glass transition temperature or in the presence of solvent, there exists a dynamic equilibrium between additive chains in the bulk and chains at the surface. The factors affecting this equilibrium are threefold; the first of which is the structure of the end group and in particular the number of CF groups and therefore the amount of fluorine present. Fluorine containing groups are known to deliver a low surface energy and this is the primary thermodynamic driving force behind surface segregation of these additives. The second factor to consider is conformational entropy; although the reduction in surface energy is the driving force for surface migration of the additives, as the surface becomes increasingly densely populated with additive molecules, the pendant chains attached to the fluoroalkyl head group need to stretch out perpendicular to the surface to allow more additive chains to accumulate at the surface. This chain stretching results in a conformational entropy penalty that must be overcome by the accompanying reduction in surface energy. At some point these two opposing effects balance each other out and no more net surface segregation occurs. However there is a third consideration that must be taken into account in explaining the relationship between additive concentration and surface properties. Small angle neutron scattering[28] has revealed the presence of large structures in the bulk of similar thin films prepared from polystyrene containing analogous additives of deuterated polystyrene and it was concluded that there is an equilibrium between free additive molecules in the bulk and aggregate structures within the bulk (see Fig. 5). Just as low molecular weight surfactants form micelles in solution upon reaching the Critical Micelle Concentration (CMC), we have shown that above a particular additive concentration the incompatibility of the fluoroalkyl end groups with the matrix polymer drives the additives to aggregate into structures in which the fluoroalkyl groups are shielded from the matrix by the pendant polymer chains. Moreover the onset of the plateau region seen in the contact angle data in Fig. 4 in fact corresponds to a Critical Aggregation Concentration (CAC) and the onset of additive aggregation. Thus further increasing the additive concentration above the CAC merely results in the formation of further aggregate structures. It is likely that only free additive chains are capable of surface migration since the rate of aggregate diffusion through the bulk will be far too slow.

Contact angle analysis – effect of matrix molecular weight

It can be seen in the contact angle data presented in figure 4a and 4b that increasing the molecular weight of the PVP matrix leads to increases in observed contact angles, particularly at concentrations below the CAC where the difference between the lowest and

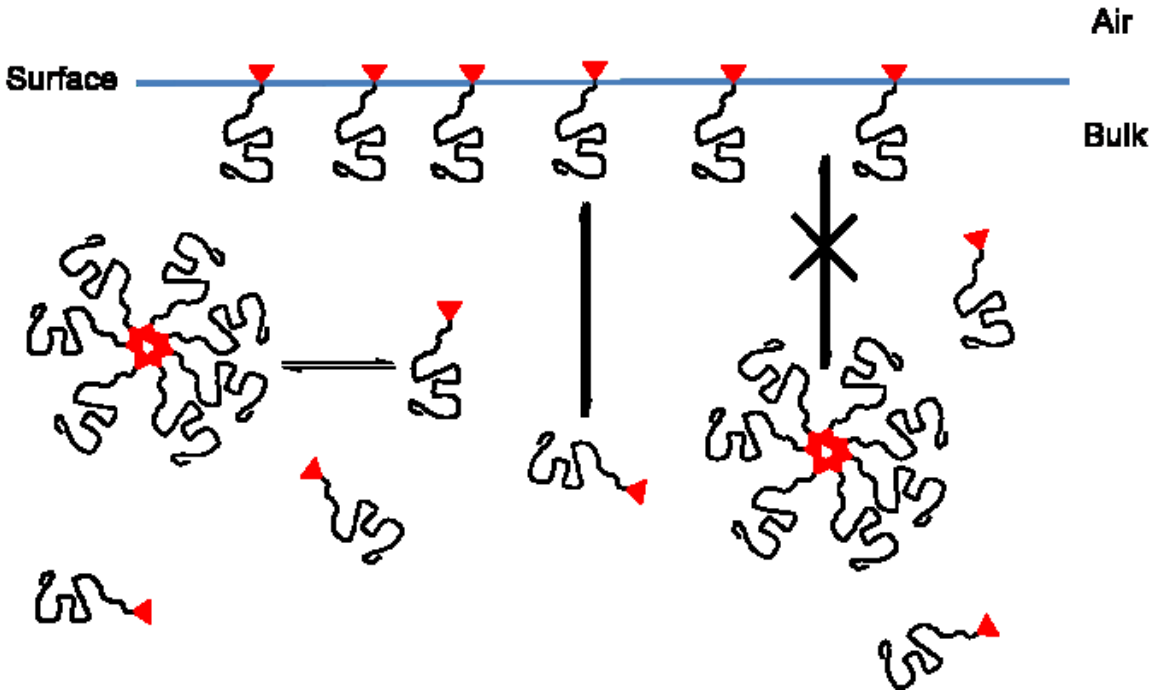

Fig. 5 Schematic depicting the behaviour of a low molecular weight polymer additive, with a pendant low surface energy end-group (red triangle), in the polymer bulk when in solution or significantly above the polymer T_g. Reproduced from Ref. 26 with permission of the Royal Society of Chemistry

highest molecular weight matrix (K15 and K90 – see table 2) can result in more than a ten degree difference in contact angle for the same concentration of additive. When considering the situation of additive concentrations below the CAC, we are no longer concerned with the equilibrium between molecularly dissolved free chains and aggregate structures, but only the equilibrium between free chains residing in the bulk or at the polymer / air interface. The increased contact angles observed with increased matrix M_n can be partly rationalised by the Flory-Huggins separation theory as applied to binary polymer blends in solution.[59-62] It is well established that the surface segregation of functional polymers in blends may be increased by incompatibility of components, since the segregation process minimises unfavourable contact between these components. For miscible blends, the entropic contribution to the free energy of mixing according to the Flory-Huggins theory decreases in magnitude with increasing degree of polymerisation, so it is perhaps not surprising that there is some increase in surface segregation observed with increasing matrix molecular weight.

Furthermore, it has also been established[63] that the discrepancy between molecular weight can also contribute to the lower molecular weight species being found in excess at the film surface. Thus a second way of visualising this behaviour relates to the ratio of additive chain ends to matrix chain ends which is obviously dependent on their respective molecular weights. Assuming that polymer chains adopt a random coil conformation, these conformations can be characterised by the root mean square end-to-end distance. Previous work has shown that in the absence of favourable interactions between monomer units and an interface or surface, there is an increase in chain end density at the surface of a polymer.[64-66].

This effect arises because there is a smaller loss of conformational entropy associated with a polymer chain end residing at the surface (which can be considered as an impenetrable boundary), when compared with the midsection of the polymer chain residing at the surface, which forces 'reflection' of the polymer chain.[64] Therefore polymer chains adjacent to the surface may adjust their conformation in order to localise their chain ends at the surface. Hence, in the case of the data in figure 4a and 4b, the impact upon surface migration of the fluoroalkyl functionality of the additive can be ignored, and the enhanced surface segregation of additive in higher M_n matrices explained by the corresponding increase in number of additive chain ends relative to the number of matrix chain ends.

Contact angle analysis – effect of additive molecular weight and type

As one might expect, the presence of the 3CFPVP6K tri-functional additive gives rise to larger increases in observed contact angles at all additive concentrations than the difunctional analogue 2CFPVP6K (see figure 4c). The molecular weight of both additives are almost identical and all other factors are constant, and these enhanced results can be attributed to the higher molar fluorine content and hence lower surface energy of the three C_8F_{17} fluoroalkyl end groups in 3CFPVP6K.

In figure 4d can be seen comparative contact angle data for three different molecular weight PVP additives carrying two fluoroalkyl groups (2CFPVP6K, 2CFPVP18K and 2CFPVP38K) PVP) in the same K15 PVP matrix. Similar qualitative trends in contact angle with increasing concentration are observed in each set of data both in terms of surface segregation and the onset of the plateau region. However, there is an obvious additional trend in behaviour across the three data sets, namely that the contact angle decreases with increasing molecular weight of the additive. These observations are consistent with studies on analogous additives of different polymer types.[27] The dominant factor to be considered in explaining this behaviour is the impact of the molecular weight of the pendant chain of the additive upon additive chain packing density at the surface. Increasing the molecular weight of the additive and hence R_G of the polymer additive will decrease the packing density of fluoroalkyl end groups at the surface. Of course the difference in molecular weight between additive and matrix will be lower for a higher molecular weight additive and the discussion above on the relative molecular weight of additive and matrix will also contribute to reduced contact angles in higher molecular weight additives. These effects combined lead to reduced surface segregation, a reduced fluorine concentration at the polymer surface, hence reduced surface lipophobicity and therefore increasing the molecular weight of the additive will give rise to lower contact angle measurements.

Contact angle analysis - annealing

Annealing of these polymer films at temperatures well in excess of the glass transition temperature of PVP should allow reorganisation of the polymer films, and past work[27,31] has shown that annealing in this fashion can result in enhanced surface segregation of polymer additives, giving rise to increased contact angle measurements. However, the temperature needs to be significantly above the T_g of the polymer in question, typically by around 40°C in these works. An extensive annealing study was performed with repeat contact angle measurements being taken from annealed films in order to try reproduce this type of result

with the PVP additives presented herein, however due to the proximity of the glass transition temperature (T_g) of K15 PVP (155°C as determined by DSC) and the onset of thermal degradation of the additive end group (175°C as determined by TGA) we were limited to annealing at a temperature of only T_g +10°C (165°C). While measurable differences in contact angles compared to equivalent unannealed films were observed, this was only the case after very long annealing times of up to 13 days, and the most prominent increase was consistently observed in 0% additive films – i.e the polymer matrix with no additive, suggesting a change in the surface unrelated to surface segregation of the additive. Surface topography of both unannealed and annealed films was investigated by means of atomic force microscopy, and it was determined that annealing has no significant effect on the surface structure of the films, which were all exceptionally smooth. A series of prolonged TGA experiments were performed on the polymer additives, in which they were held at the annealing temperature of 165°C for four days in order to ascertain whether thermal degradation was occurring over these prolonged time periods, which it did not appear to be. Given insignificant changes in surface roughness (as determined by AFM), we suspect that thermal degradation may be responsible for any changes in contact angle as a result of annealing and the unavoidable proximity between the annealing temperature and the measured onset of thermal degradation. Whilst this could be proven by the TGA, the huge surface area to volume ratio of a 250nm thick polymer film renders it more susceptible to heat than a powdered TGA sample.

Rutherford backscattering analysis

While contact angle analysis is a facile and informative method of characterising surface properties, it is an indirect method and the resulting contact angles arise as a result on both surface chemistry and surface topography. Therefore contact angle analysis can give no quantitative information on the extent of fluorine enrichment at the surface. In order to quantitatively measure this, grazing angle Rutherford backscattering (RBS)[67,68] was used to analyse a set of polymer films containing varying concentrations of 2CFPVP6K additive. An incident beam of monoenergetic, high energy $^4He^+$ ions was brought onto the sample at a grazing angle of 4.6°, meaning the beam which penetrates a certain depth into the sample, only interacts with the top few layers of atoms in the sample surface. Backscattered ions lose energy through discrete interactions with electrons and via collisions with target nuclei and the atomic mass of the target nuclei directly affects the energy of the backscattered ion. In this way RBS can detect not only backscattered ions, but by measuring their energy it can identify the element with which a collision event occurred. RBS is more sensitive to the presence of heavier elements due to their larger nuclei and the associated increased probability of a collision event. However RBS is better at differentiating between lighter elements as the difference between their atomic masses is more significant relative to their atomic masses, thus signals are easier to resolve from one another. This makes RBS particularly sensitive to the presence of fluorine in PVP since the atomic mass of fluorine is higher than all of the lighter elements comprising the polymer (C, N and O – H is not relevant as it is incapable of backscattering an ion of greater mass than its own). The fluorine peak arising from its presence at the surface of the polymer film is easily resolvable, being detected at 570 keV as in previous cases[27]. By normalising recorded data using the known

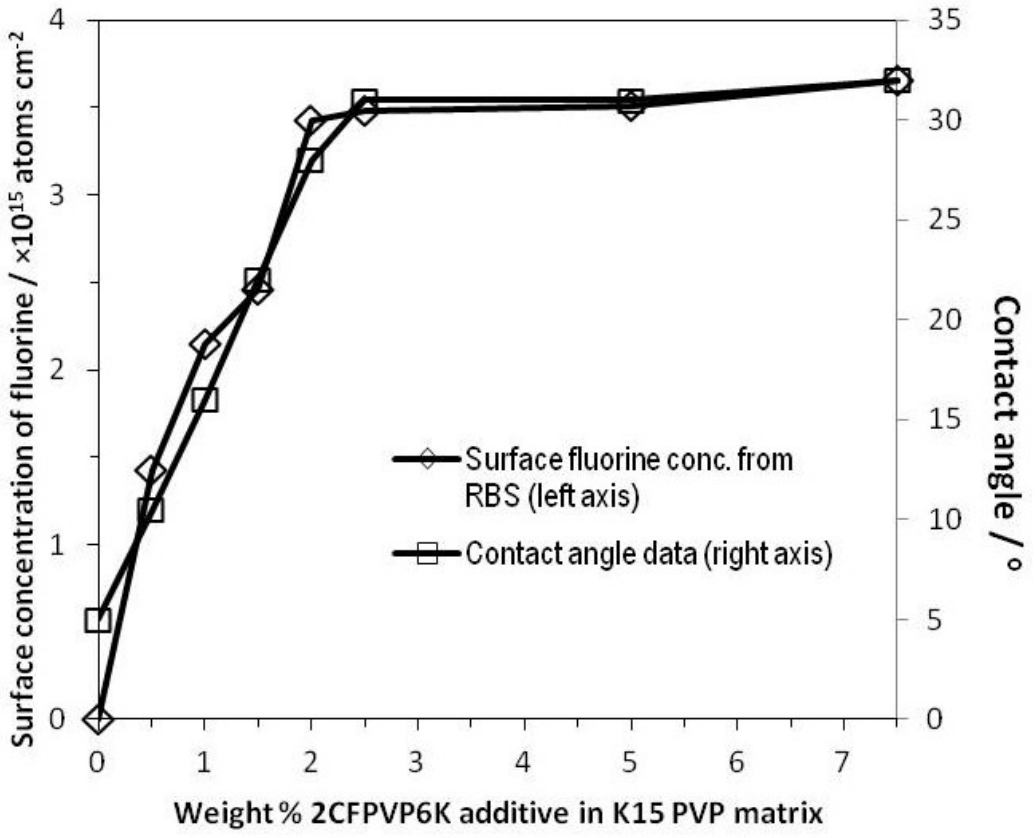

Figure 6. Plot of 2CFPVP6K additive concentration in a K15 PVP matrix against surface concentration of fluorine atoms as determined by RBS (left axis), and contact angle analysis (right axis).

concentration of carbon in the sample, and subsequent integration of the fluorine peak, the concentration of fluorine atoms at the surface can be directly measured. This data analysis was performed with the SIMNRA program.[69] The resulting data (figure 6) is complementary to the corresponding contact angle data, and it has been overlaid with a secondary axis to illustrate this. It can clearly be seen that the RBS analysis of this series of PVP films correlates very well with the corresponding contact angle data, with the plateau region corresponding to the CAC being arrived at the same concentration of additive. This RBS data also confirms that the increase in contact angle as a function of additive concentration can be attributed directly to an increase in the concentration of fluorine at the surface.

Conclusions

We describe here the synthesis of two novel, functionalised chain transfer agents for the RAFT polymerisation of *N*-vinyl pyrrolidone, and their subsequent use in the synthesis of a series of multi-end functionalised polymer additives, bearing end groups possessing two or three C_8F_{17} fluoroalkyl groups. These low molecular weight polymer additives are designed to modify the surface of ordinary PVP, by means of spontaneous surface segregation when in

the presence of solvent, facilitated by the low surface energy of the pendant fluoroalkyl chains. Both of the di-functional and tri-functional PVP additives were prepared with molecular weights ranging from 5,000 to 50,000 g mol^{-1}. We have reported, that in accordance with previous work involving analogous additives made from differing polymeric materials, that increasing the number of fluoroalkyl chains in the end group, or increasing the concentration of additive up to the critical aggregation concentration results in a lowering of the polymer surface energy, and therefore increased lipophobicity. We have also described the impact of additive molecular weight relative to that of the PVP matrix whereby an increase in the matrix molecular weight relative to that of the additive resulted in enhance surface migration of the additive and increased surface lipophobicity. We have shown that these additives dispersed in a polymer matrix behave in a similar fashion to surfactants in solution, existing as surface active, molecularly dissolved free chains until they are present in such a concentration that they spontaneously form aggregate structures within the bulk in preference to further surface adsorption. The concentration at which this occurs, termed the 'critical aggregation concentration' can be observed in the contact angle data presented, as the onset of a plateau region, where further increases in concentration of additive have no further effect on observed contact angles. This behaviour is in contrast to the assumption that the onset of a plateau corresponds to surface saturation of the additive as dictated by the physical size of additive molecules and their maximum packing density, which would in theory give rise to a similar plateau region. This has been shown to not be the case in previous work where upon annealing of polymer films containing analogous additives has led to enhanced surface segregation, strongly implying that the surface concentration of additive is in fact dictated by the more complex dynamic equilibrium between free chains and aggregate structures as described above. An extensive annealing study was undertaken with the PVP additives presented herein, though it was unsuccessful owing to the unavoidable proximity between the higher T_g of the PVP matrix and the onset of thermal degradation of the additive end group. RBS was used to quantitatively measure the concentration of fluorine at the polymer surface of a series of polymer blends incorporating a low molecular weight di-functional additive, which is a more direct method of measuring the concentration of fluorine at the near surface, and hence the extent of surface segregation, than contact angle analysis. RBS data was in correlated very strongly with contact angle data, showing the onset of a plateau region at exactly the same concentration of additive, corresponding to the preferential formation of aggregate structures over further surface adsorption.

Acknowledgements

We gratefully acknowledge the support of Technical Fibre Products Ltd., and the UK Engineering and Physical Sciences Research Council (EPSRC) for joint-funding the PhD studies of Dr Bergius. We also acknowledge the financial support of the Malaysian Government and The University of Malaya for funding the PhD studies of Dr Muhamad-Sarih and support from the Department of Chemistry, Durham University.

References

1. H. S. Kollisch, C. Barner-Kowollik and H. Ritter, *Chemical Communications*, 2009, 1097.
2. P. E. Millard, L. Barner, J. Reinhardt, M. R. Buchmeiser, C. Barner-Kowollik and A. H. E. Muller, *Polymer*, 2010, **51**, 4319.
3. A. Walther, P. E. Millard, A. S. Goldmann, T. M. Lovestead, F. Schacher, C. Barner-Kowollik and A. H. E. Muller, *Macromolecules*, 2008, **41**, 8608.
4. A. Gregory and M. H. Stenzel, *Progress in Polymer Science*, 2012, **37**, 38.
5. C. B. Zhang, Y. A. Zhou, Q. A. Liu, S. X. Li, S. Perrier and Y. L. Zhao, *Macromolecules*, 2011, **44**, 2034.
6. D. Konkolewicz, M. J. Monteiro and S. Perrier, *Macromolecules*, 2011, **44**, 7067.
7. B. L. Liu, A. Kazlauciunas, J. T. Guthrie and S. Perrier, *Macromolecules*, 2005, **38**, 2131.
8. M. A. Tasdelen, M. U. Kahveci and Y. Yagci, *Progress in Polymer Science*, 2011, **36**, 455.
9. G. Moad, E. Rizzardo and S. H. Thang, *Polymer International*, 2011, **60**, 9.
10. H. Willcock and R. K. O'Reilly, *Polymer Chemistry*, 2010, **1**, 149.
11. C. Barner-Kowollik, *Handbook of RAFT Polymerization*, Wiley-VCH, 2008.
12. G. Kostov, F, Boschet, J. Buller, L. Badache, S. Brandsadter and B. Ameduri. *Macromolecules*, 2011, **44**, 1841.
13. P. Lebreton, B. Ameduri, B. Boutevin and J. M. Corpart. Macromol. Chem. Phys., 2002, **203**, 522.
14. L. J. Ward, J. P. S. Badyal, A. J. Goodwin and P. J. Merlin, *Polymer*, 2005, **46**, 3986.
15. F. Montefusco, R. Bongiovanni, A. Priola and B. Ameduri, *Macromolecules*, 2004, **37**, 9804
16. B. Ameduri, R. Bongiovanni, V. Lombardi, A. Pollicino, A. Priola and A Recca, *J. Polym. Sci., Part A: Polym. Chem.*, 2001, **39**, 4227.
17. B. Ameduri, R. Bongiovanni, G. Malucelli, A Pollicino and A Priola, *J. Polym. Sci., Part A: Polym. Chem.*, 1999, **37**, 77.
18. R. Bongiovanni, N, Pollicino, G. Gozzelino, G. Malucelli, A. Priola, and B. Ameduri, *Polym. Adv. Technol.*, 1996, **7**, 403.
19. F. T. Kiff, R. W. Richards and R. L. Thompson, *Langmuir*, 2004, **20**, 4465.
20. L. R. Hutchings, R. W. Richards, R. L. Thompson and D. G. Bucknall, *European Physical Journal E*, 2002, **8**, 121.
21. J. T. Koberstein, *J. Polym. Sci., Part B: Polym. Phys.*, 2004, **42**, 2942.
22. P. A. V. O'Rourke Muisener, C. A. Jalbert, C. Yuan, J. Baetzold, R. Mason, D. Wong, Y. J. Kim and J. T. Koberstein, *Macromolecules*, 2003, **36**, 2956.
23. P. A. V. O'Rourke Muisener, J. T. Koberstein and S. Kumar, *Macromolecules*, 2003, **36**, 771.
24. L. R. Hutchings, R. W. Richards, R. L. Thompson, D. G. Bucknall and A. S. Clough, *Eur. Phys. J. E.*, 2001, **5**, 451.
25. I. Hopkinson, F. T. Kiff, R. W. Richards, D. G. Bucknall and A. S. Clough, *Polymer*, 1997, **38**, 87.
26. T. F. Schaub, G. J. Kellogg, A. M. Mayes, R. Kulasekere, J. F. Ankner and H. Kaiser, *Macromolecules*, 1996, **29**, 3982.
27. L. R. Hutchings, N. M. Sarih and R. L. Thompson, *Polymer Chemistry*, 2011, **2**, 851.
28. I. A. Ansari, N. Clarke, L. R. Hutchings, A. Pillay-Narrainen, A. E. Terry, R. L. Thompson and J. R. P. Webster, *Langmuir*, 2007, **23**, 4405.
29. L. R. Hutchings, A. P. Narrianen, R. L. Thompson, N. Clarke and L. Ansari, *Polymer International*, 2008, **57**, 163.

30. R. L. Thompson, A. P. Narrainen, S. M. Eggleston, I. A. Ansari, L. R. Hutchings and N. Clarke, *Journal of Applied Polymer Science*, 2007, **105**, 623.
31. A. P. Narrainen, L. R. Hutchings, I. Ansari, R. L. Thompson and N. Clarke, *Macromolecules*, 2007, **40**, 1969.
32. A. L. Narrainen, L. R. Hutchings, I. A. Ansari, N. Clarke and R. L. Thompson, *Soft Matter*, 2006, **2**, 126.
33. L. R. Hutchings, A. P. Narrainen, S. M. Eggleston, N. Clarke and R. L. Thompson, *Polymer*, 2006, **47**, 8116.
34. S. M. Kimani, S. J. Hardman, L. R. Hutchings, N. Clarke and R. L. Thompson, *Soft Matter*, 2012, **8**, 3487.
35. S. J. Hardman, L. R. Hutchings, N. Clarke, S. M. Kimani, L. L. E. Mears, E. F. Smith, J. R. P. Webster and R. L. Thompson, *Langmuir*, 2012, **28**, 5125.
36. T. S. Cheng, H. T. Lin and M. J. Chuang, *Mater. Lett.*, 2004, **58**, 650.
37. E. Selli, G. Mazzone, C. Oliva, F. Martini, C. Riccardi, R. Barni, B. Macandalli, and M. R. Massafra, *J. Mater. Chem.*, 2001, **11**, 1985.
38. S. Sigurdsson and R. Shishoo, *J. Appl. Polym. Sci.*, 1997, **66**, 1591.
39. T. Kawase and H. Sawada, *J. Adhes. Sci. Technol.*, 2002, **16**, 1121.
40. T. Kawase, M. Yamane, T. Fugi and M. Minigawa, *J. Adhes. Sci. Technol.*, 1997, **11**, 1381.
41. S. Biltresse, D. Deschamps, T. Boxus and J. Marchand-Brynaert, *J. Polym. Sci., Part A: Polym. Chem.*, 2000, **38**, 3510.
42. D. L. Schmidt, C. E. Coburn, B. M. DeKoren, G. E. Potter, G. F. Meyers and D. A. Fischer, *Nature*, 1994, **368**, 39.
43. F. Saïdi, F. Guittard, C. Guimon and S. Géribaldi, *Macromol. Chem. Phys.*, 2005, **206**, 1098.
44. S. J. Hardman, N. Muhamad-Sarih, H. J. Riggs, R. L. Thompson, J. Rigby, W. N. A. Bergius and L. R. Hutchings, *Macromolecules*, 2011, **44**, 6461.
45. D. Charmot, P. Corpart, D. Michelet, S. Zard and T. Biadatti, *Chem. Abstr.*, 1999, **130**, 82018.
46. G. Moad, E. Rizzardo, S. H. Thang, *Aust. J. Chem.*, 2005, **58**, 379.
47. S. Z. Zard, *Aust. J. Chem.*, 2006, **59**, 663.
48. R. Devasia, R. L. Bindu, R. Borsali, N. Mougin and Y. Gnanou, *Macromol. Symp.*, 2005, **229**, 8.
49. P. Bilalis, M. Pitsikalis and N. Hadjichristidis, *J. Polym. Sci., Part A: Polym. Chem.*, 2006, **44**, 659.
50. A. K. Mishra, V. K. Patel, N. K. Vishwakarma, C. S. Biswas, M. Raula, A. Misra, T. K. Mandal and B. Ray, *Macromolecules*, 2011, **44**, 2465.
51. A. Guinaudeau, S. Mazières, D. J. Wilson and M. Destarac, *Polym. Chem.*, 2012, **3**, 81.
52. M. Vivek and K. Rajesh, *Journal of Applied Polymer Science*, 2012, **124**, 4475
53. G. Pound, F. Aguesse, J. B. McLeary, R. F. M. Lange and B. Klumperman, *Macromolecules,* 2007, **40**, 8861
54. N. Bailly, G, Pound-Lana and B, Klumperman, *Aust. J. Chem.* 2012, **65**, 1124.
55. M. K. Georges, R. P. N. Veregin, P. M. Kazmaier and G. K. Hamer, *Macromolecules*, 1993, **26**, 2987.
56. J. Hawker, A. W. Bosman and E. Harth, *Chem. Rev.*, 2001, **101**, 3661.
57. Y. K. Chong, T. P. T. Le, G. Moad, E. Rizzardo and S. H. Thang, *Macromolecules*, 1999, **32**, 2071.
58. J. B. Hudson, *Surface Science: An Introduction*, Wiley-Interscience, 1998, 63–65.
59. M. L. Huggins, *J. Chem. Phys.*, 1941, **9**, 440.

60. P. J. Flory, *J. Chem. Phys.*, 1941, **9**, 660.
61. C. Qian, S. J. Mumby and B. E. Eichinger, *Macromolecules*, 1991, **24**, 1655.
62. B. M. Forrest and R. Toral, *Journal of Statistical Physics*, 1994, **77**, 473.
63. A. Hariharan, S. K. Kumar and T. P. Russell, *Journal of Chemical Physics*, 1993, **98**, 4163.
64. K. A. Welp, R. P. Wool, G. Agrawal, S. K. Satija, S. Pispas and J. Mays, *Macromolecules*, 1999, **32**, 5127.
65. A. M. Botelho do Rego and J. D. Lopes da Silva, *Macromolecules*, 1993, **26**, 4986.
66. W. Zhao, X. Zhao, M. H. Rafailovich and J. Sokolov, *Macromolecules*, 1993, **26**, 561.
67. R. J. Composto, R. M. Walters and J. Genzer, *Mater. Sci. Eng. R*, 2002, **38**, 107.
68. M. Nastasi and J. R. Tesmer, *Handbook of Modern Ion Beam Materials Analysis*, Materials Research Society, 1995.
69. M. Mayer, *SIMNRA User's Guide*, Max-Planck-Institut für Plasmaphysik, 2002.

[a] *Department of Chemistry, Durham University, Durham, United Kingdom, DH1 3LE. Fax: +44 191 334 2051; Tel: +44 191 334 2133; E-mail:l.r.hutchings@durham.ac.uk*
[b] *Chemistry Department, Faculty of Science, University of Malaya, 50603 Kuala Lumpur, Malaysia*
[c] *Technical Fibre Products Limited, Burneside Mills, Kendal, Cumbria, United Kingdom, LA9 6PZ.*

Graphical Abstract

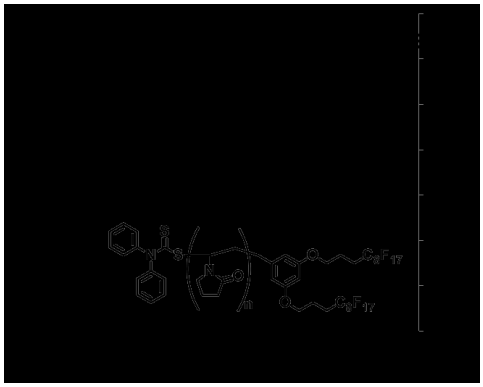

Fluoroalkyl end-functionalized poly(*N*-vinylpyrrolidone) additives prepared by RAFT polymerisation with functionalized transfer agents undergo spontaneous surface migration to modify surface properties. Surface elemental composition data (ion beam analysis) correlates extremely well with static contact angle analysis.